**Charles University in Prague**

**Faculty of Science**

Institute of Hydrogeology, Engineering Geology and Applied Geophysics

Study program: Geology

Field of study: Geotechnology


**Dayansetsen Boldbaatar**

# Evaluation of rock masses on planetary surfaces

Určování hmotnosti kamenů (valounků) na povrchu planet

Bachelor's thesis

Thesis supervisor: doc. RNDr. Günther Kletetschka, Ph.D.

Prague, 2020

**Univerzita Karlova v Praze**

**Přírodovědecká fakulta**

Ústav hydrogeologie, inženýrské geologie a užité geofyziky

Studijní program: Geologie

Studijní obor: Geotechnologie


**Dayansetsen Boldbaatar**

# Určování hmotnosti kamenů (valounků) na povrchu planet

# Evaluation of rock masses on planetary surfaces

Bakalářská práce

Vedoucí práce/školitel: doc. RNDr. Günther Kletetschka, Ph.D.

Praha, 2020

Prohlašuji, že jsem závěrečnou práci zpracoval samostatně a že jsem uvedl všechny použité informační zdroje a literaturu. Tato práce ani její podstatná část nebyla předložena k získání jiného nebo stejného akademického titulu.

Declaration:

I, Dayansetsen Boldbaatar, hereby declare that I worked out this bachelor thesis alone and that all the information sources and literature are cited. Entire thesis or any part of it has not been submitted to obtain the same or other academic degree.

Prague, July 15, 2020

V Praze, 15.7.2020

Signature/Podpis: ……/ Dayansetsen Boldbaatar/

SUMMARY

The understanding of rock mass has great benefits in engineering and geology. This understanding can benefit in the field of colonizing and terraforming other planetary bodies. To achieve this task, we can begin by using current methods to see if we can evaluate rock mass and if these can be inferred to understanding rock mass on other planetary bodies.

Therefore, this bachelor's thesis is sought to examine if the use of compositional and volume information in order to figure out the mass of a rock pebbles on planetary bodies. For this purpose, 3D computing Photogrammetry method and X-ray Fluorescence methods were used to derive the necessity physical quantities for the mass computing.

Five rocks where used in this study. Data was collected and analyzed using the two methods, software program and instruments. The results showed use of the two methods were accurate and efficient. Compare to the classic methods, these two methods proved as efficient and accurate.

ABSTRAKT

Pochopení horninové hmoty má velké výhody v inženýrství a geologii. Toto porozumění může být přínosem v oblasti kolonizace a terraformování jiných planetárních těl. K dosažení tohoto úkolu můžeme začít pomocí současných metod, abychom zjistili, zda můžeme vyhodnotit hmotnost horninu a zda je lze odvodit z pochopení horninového masa na jiných planetárních tělesech.

Cílem této bakalářské práce je proto prozkoumat, zda použití informací o složení a objemu k určení hmotnosti hornin na planetárních tělesech. Za tímto účelem byly k odvození nezbytných fyzikálních veličin pro hromadné výpočty použity metody 3D počítačové fotogrametrie a rentgenové fluorescenční metody.

V této studii bylo použito pět hornin. Data byla sbírána a analyzována pomocí dvou metod, softwarového programu a nástrojů. Výsledky ukázaly, že použití těchto dvou metod bylo přesné a efektivní. Ve srovnání s klasickými metodami se tyto dvě metody osvědčily efektivní a přesné.

ACKNOWLEDGEMENTS

I would like to thank to my supervisor doc. RNDr. Günther Kletetschka, Ph.D. for dedicating his time on valuable consultations, corrections, patient reviews and for tolerant acceptance of supervising. I am also grateful to my colleagues Chipo Malambo, Yunden Tuvshinbayar, Viťa Malčík for the support. Finally, I would like to thank to Uuriintsolmon Dunbulag and my family also friends for encouraging and supporting all this time.

# Table of Contents

# 1. INTRODUCTION

Colonization and terraforming of other planetary bodies require an understanding of such planetary surfaces which still is a challenge. One of the ways we can understand this is by evaluating the rock masses of these planetary bodies. It is important to understand that, as data has shown that rock mass on different planetary bodies will differ due to the gravity and rock composition. However, by perfecting our techniques in understanding and evaluating rock mass by using earth rocks as in this study, we can use these same techniques to understand rock mass from other planetary bodies.

The work in this thesis focuses on using two techniques such as volume computing photogrammetry and density determination by x-ray fluorescence, to evaluate 5 rocks and their masses. The main purpose of this work was to investigate and show that these techniques can be used to evaluate rock mass and probably use the same techniques to understand rock mass from other planetary surfaces.

In this study 5 rocks from Saratoga Springs in the United States were used.

The first part of the work gives a general overview of rocks and rock mass. The second part uses the Moon as an example of a planetary body and gives a summary of the Moon and its properties, how would they influence colonizing and terraforming. The thesis goes on to definitions of the techniques used in this study. The thesis ends with the methodology, results, and the discussion, conclusion are given.

# 2. DEFINITION OF ROCK

Rocks can be characterized to be composed of at least one mineral and/or glass (glass is not a mineral). As indicated by the procedure of development, rocks can be partitioned into three significant classes. These include:

(1) igneous rocks, which have solidified from the molten material called magma;

(2) sedimentary rocks, those consisting of fragments derived from the preexisting rocks or of minerals precipitated from the solutions;

(3) metamorphic rocks, which have been derived from either igneous or sedimentary rocks under conditions that caused changes in their mineralogical composition, texture, and internal structure (Carmichael, 2017).

These three classes are additionally partitioned into various gatherings and types based on different components, the most significant of which are:

chemical,

mineralogical,

and textural attributes (Carmichael, 2017).

## 2.1. Rock Mass

Rock mass is a matrix consisting of rock material and rock discontinuities. Its classification and characterization allows mapping the rock boundaries (Singh & Goel, 1999).

## 2.2. Parameters used in rock mass classification

The following are the most significant parameters that are used in classification systems:

- Strength and deformability of intact rock
- Rock Quality Designation (RQD) which considers the intensity of fracturing in a drill core
- Rock fractures parameters (spacing, orientation, width, roughness, weathering, etc.)
- Groundwater pressure and flow

- In-situ stress
- Geological structures such as faults and folds (Singh & Goel, 1999).

Benefits of understanding Rock Mass

These are number of reasons to classifying and understanding rock mass. Some of the reasons are as follows

1. They give a foundation for understanding the characteristics of each rock
2. They help in engineering, by helping make better judgement and effective communication during a project
3. It is important for quantitative information and design purposes
4. Improving the quality of site investigations by calling for the minimum input data as classification parameters (Bieniawski, 1993).

# 3. MOON

In this work, the Moon is used as an example of a planet whose rocks can be used to measure rock mass on its surface. As earlier mentioned, the rocks used for this study are from the earth but based on the laboratory work and results, these techniques can used on the Moon to give us a better understanding of rock mass on the moon. Following is general outlook of the moon and its properties.

The Moon is a unique satellite that is considered the fifth largest satellite in the Solar System with 3474 km diameter and has a surface gravity to 1.622 $m/s^2$, about 17% of that on Earth. Its surface area is less than $1/10^{th}$ of the Earth's surface, volume is about 2%, mass with only 1.2% of that of Earth, and rotates on its axis once every 27.3 days. Due to strain produced in a celestial body that undergoes cyclic variations in gravitational attraction (tidal friction) with deformations, lunar rotation slowed down and became locked into a synchronous state, orienting the Moon such that the same hemisphere faces the Earth at all times. Most of our insight into the Moon depends on the observation made using telescopes from Earth, remote sensing, measurements on the lunar surface by manned and unmanned landed missions and the examinations of lunar examples including those returned by the Apollo and Luna missions, also lunar meteorites found on Earth (Jaumann et al., 2012).

## 3.1. Lunar morphology and stratigraphy

The Moon's core is relatively smaller than other earthly bodies cores. The strong, iron-rich internal core is 240 kilometers in diameter, mostly liquid layer with a thickness of 150 kilometers encompasses the iron center. The mantle extends from the top of the partially molten layer to the bottom of the Moon's crust. It is in all probability made of minerals like olivine and pyroxene, which are comprised of magnesium, iron, silicon and oxygen particles. The outside has a thickness of around 70 kilometers on the Moon's near side of the equator and 150 kilometers on the far-side. It is made of oxygen, silicon, magnesium, iron, calcium and aluminum, with limited quantities of titanium, uranium, thorium, potassium and hydrogen. Long ago the Moon had active volcanoes, but today they are all dormant and have not erupted for millions of years and with too meager an atmosphere to obstruct impacts, a consistent downpour of space rocks, meteoroids and comets strikes the surface of the Moon, deserting various craters, that, one of the crater is Tycho Crater is

more than 85 kilometers wide. More than billions of years, these impacts have ground up the outside of the Moon into segments running from colossal stones to dust (McFadden et al., 2007).

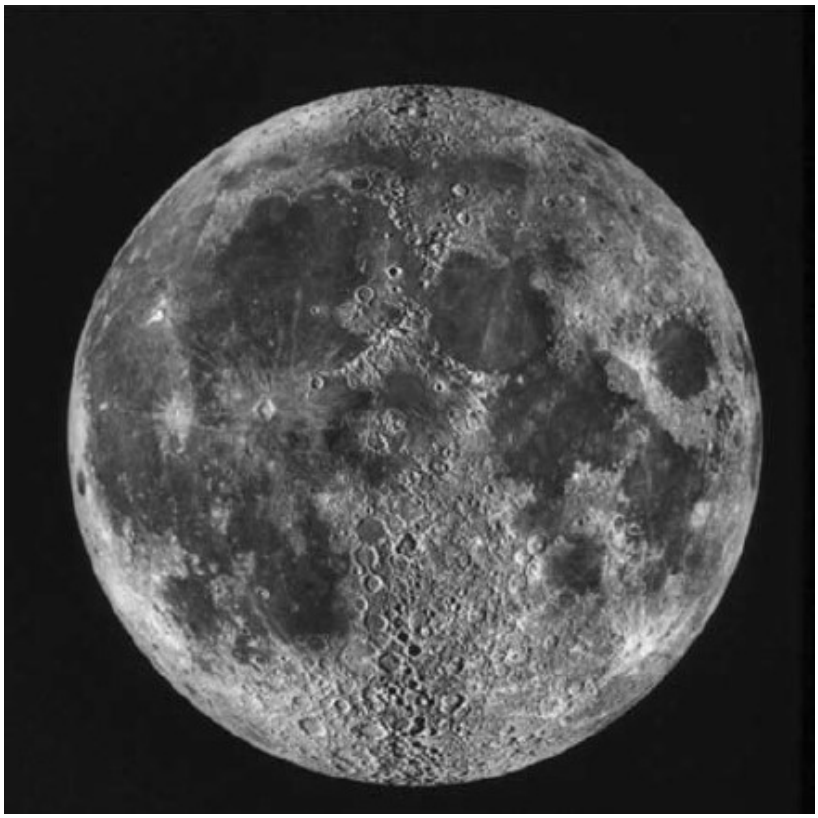

*Figure 1. A composite full-Moon photograph that shows the contrast between the heavily cratered highlands and the smooth, dark basaltic plains of the maria (McFadden et al., 2007).*

According to the NASA Solar system exploration information these light areas of the Moon are known as the highlands. In the range of 4.2 and 1.2 billion years back these basins were filled with lava and those dark highlights are called mare (Latin for seas). These light and dim zones speak to rocks of various organization and ages, which give proof to how the early outside layer may have crystallized from a lunar magma ocean. The craters themselves, which have been saved for billions of years, illuminate the history to the moon and different bodies in the internal nearby planetary group.

In compliance with Wilhelm (1987) and Stoffler and Ryder (2001) as cited in (Jaumann et al., 2012), stratigraphically and chronologically the Moon is divided into five time periods: Pre-Nectarian (>3.92/4.1 Ga), Nectarian (3.92/4.1-3.85/3.91 Ga), Imbrian (3.85/3.91-3.2 Ga),

Eratosthenian (3.2-1.0/0.8 Ga), and Copernican (<1.0/0.8 Ga). The formal stratigraphic sequence is given in Table 1.

*Table 1. Formal stratigraphic sequence (McFadden et al., 2007).*

| System | Age (billion years) | Remarks |
|---|---|---|
| Copernican | 1.0 to present | The youngest system, which includes fresh ray craters (e.g., Tycho), begins with the formation of Copernicus. |
| Eratosthenian | 1.0–3.1 | Youngest mare lavas and craters without visible rays (e.g., Eratosthenes). |
| Imbrium | 3.1–3.85 | Extends from the formation of the Imbrium Basin to the youngest dated mare lavas. Includes Imbrium Basin deposits, Orientale and Schrödinger multiring basins, most visible basaltic maria, and many large impact craters, including those filled with mare lavas (e.g., Plato, Archimedes). |
| Nectarian | 3.85–3.92 | Extends from the formation of the Nectaris Basin to that of the Imbrium Basin. Contains 12 large, multiring basins and some buried maria. |
| Pre-Nectarian | Pre-3.92 | Basins and craters formed before the Nectaris Basin. Includes 30 identified multiring basins. |

### 3.2. Lunar crust

Lunar highlands are mainly formed by anorthositic rocks and plagioclase-rich magnesian-suite rocks including norites, gabbronorites, and troctolites and KREEP basalts are found among the Apollo missions. The Moon's ~ 60% surface area and is composed primarily of ancient anorthositic rocks presumed to be mainly of the ferroan anorhositic suite and magnesian-suite rocks make up approximately 20% of the Moon crust.

Laboratory studies revealed that the lunar samples can be classified into four distinct groups:

(1) pristine highland rocks that are primordial igneous rocks;

(2) pristine basaltic volcanic rocks, including lava flows and pyroclastic deposits;

(3) polymict clastic breccias, impact melt rocks;

(4) the lunar regolits and regolith breccias (Jaumann et al., 2012).

Lunar Prospector data indicate that KREEP-rich rocks are abundant around Imbrium basin, thus, most highland rocks were formed during the differentiation of a magma ocean. During the heavy

bombardment ~ 4.1-3.8 Ga, numerous large impacts shattered and fragmented the lunar crust down producing a global layer of mixed impact debris, called “megaregolith” (Jaumann et al., 2012).

#### 3.2.1. Lunar rocks compared to earth rocks

Almost all the rocks at the lunar surface are igneous—they formed from the cooling of lava. On the other hand, the most common rocks on Earth’s surface are sedimentary, which required the activity of water or wind for their development. The two most common kinds are basalts and anorthosites. The lunar basalts, relatively rich in iron and many also in titanium, are found in the maria. In the highlands the rocks are largely anorthosites, which are relatively rich in aluminum, calcium, and silicon (Burke, 1986).

While the greater part of the minerals in Moon rocks are found on Earth, they were framed in totally different situations. Moon rock shows proof of arrangement in an amazingly dry setting, with low gravitational impact and with to no oxygen. This is completely different to the Earth’s environment at the time of formation, approximately between three to four-and-a-half billion years ago. Lunar rocks also contain trapped gases from the solar wind passing them at the time of formation (Burke, 1986).

These differences are highlighted to ensure that before terraforming a planetary body such as the moon, we exactly know what rock type we are evaluating for mass. As mentioned above rock mass has a critical importance when making engineering judgement. By understanding and evaluating rock mass on our own planet, we can perfect these techniques and make inferences on other planetary bodies.

### 3.3. Lunar internal structure

The lunar interior is critical to better understanding the development, separation, and advancement of the early Solar System as a rule and the Earth-Moon framework specifically. Lunar density of 3344 $kg/m^3$ demonstrates that the Moon has just a little iron core contrasted with that of Earth or some other earth-like planet. As cited in (Jaumann et al., 2012) according to the papers of Zuber (1994), Araki (2009) and Scholten (2012) the worldwide models of lunar topography have improved as far as spatial resolution and accuracy, as well as precise laser altimetry-based maps and improved coverage with sound system pictures became accessible.

### 3.3.1.Lunar seismicity

Other than Earth, Moon is the only body that, broad seismological examinations were driven adequately. With the assistance of the space travelers introducing long period seismometers on the Moon from the four missions of Apollo, according Zhao et.al., (2008, 2012) as cited in (Steinberger et al., 2015), yet as of the late this seismic data has been used to construct a lunar tomographic model (Fig. 2). Lunar network distinguished in excess of 13000 seismic occasions, that these information's assessment and discussion proceed at the present time. It was discovered that, from this given information, the lunar seismicity is on a very basic level not quite the same as that of the Earth attributable to the absence of tectonic plate movement. Seismic sources on the Moon can be grouped in three principle classifications: the deep moonquakes, shallow moonquakes, and meteoroid impacts (Jaumann et al., 2012).

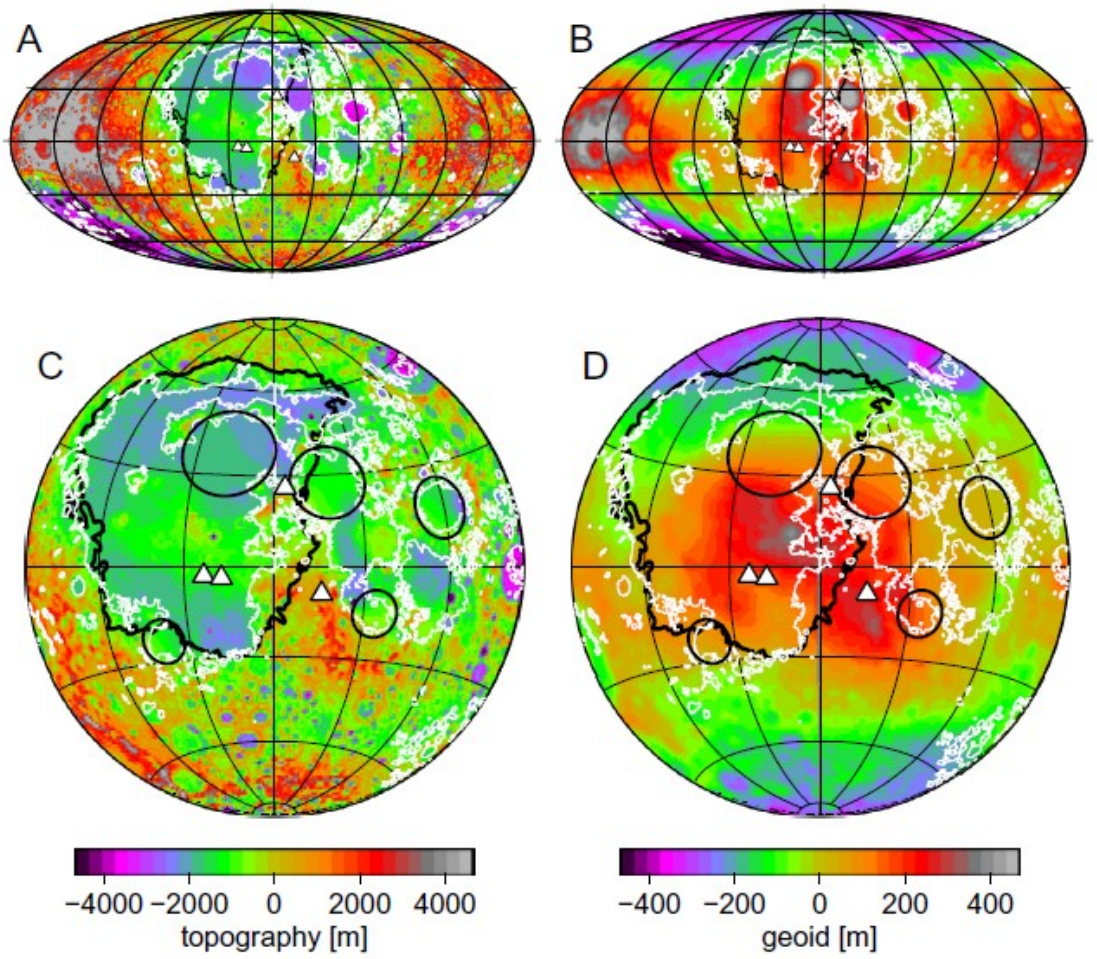


*Figure 2. Figure 2. Topography and gravity equipotential surface are shown in A and B. In B geoid highs are shown associated with five nearside ringed maria (Imbrium, Serenitatis, Crisium, Nectaris, and Humorum). In C and D is shown interpolated geoid and topography inside the mascons from surrounding values. Triangles indicate Apollo seismometer locations and Procellarum KREEP terrane is outlined in black (Steinberger et al., 2015).*

According to Nakamura, (2005, 2008), as cited in (Jaumann et al., 2012), deep moonquakes happen in supposed "nests" which more than once discharge seismic vitality in explicit cycles corresponded with the lunar tides. More than 7000 individual profound moonquakes could be doled out to one of the more than 250 of these homes, which are arranged at profundities somewhere in the range of 700 and 1100 km. The shallow lunar quakes stay confounding, that, they are solid contrasted with the profound moonquakes; however generally uncommon. Their epicenters were not associated with known geological highlights and this sort of moonquake likely speaks to the arrival of thermoelastic stresses in the lunar outside layer or the upper mantle and may be associated with large impact basins (Nakamura, 1979 & Oberst, 1987 as cited in Jaumann et al., 2012).

### 3.3.2.Lunar gravity

The Gravitational field of the Moon gives significant data on the spatial conveyance of mass at the surface and inside the lunar inside. According to Akim, 1966, as cited in (Konopliv et al., 1998), the gravity field of the moon has been investigated since 1966 when the Russian Luna 10 was put in circle around the Moon and gave dynamical verification that the oblateness of the moon's gravitational potential points out that there was larger than the shape predicted from hydrostatic equilibrium. Resulting, huge nearside mass concentration, purported mascons, from view Doppler following information of Lunar Orbiter V were found (Muller & Sjorgren, 1968 as cited in Wirnsberger et al., 2019).

According to Matsumoto, (2009) & Namiki, (2009) as cited in (Jaumann et al., 2012), with one satellite put in a high circle as a transfer satellite between the fundamental orbiter and the Earth and a VLBI subsatellite for differential following of the relay satellite, embedded in coplanar polar circles, along these lines impressively improving the medium-to-short-scale lunar gravitational field arrangement was accomplished by Kaguya-Selene as the first reliable gravity field determination for the lunar far side. However, the data substance of the farside is as yet limited the principal committed gravity mission in planetary science, the Gravity Recovery and Interior Laboratory (GRAIL) (Zuber, (2013) as cited in Wirnsberger et al., 2019), supersedes prior missions in view of revealing a global lunar gravity field. The twin-satellite crucial of "Ebb" and "Flow" understood a low-low following setup with a Ka-band inter satellite connection.

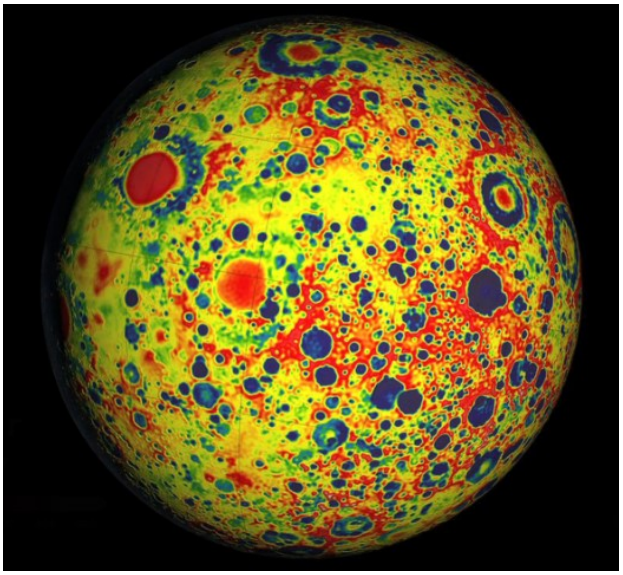

*Figure 3. Variations in the lunar gravity field as measured by NASA's Gravity Recovery and Interior Laboratory (GRAIL). The field shown resolves blocks on the surface of about 20 kilometers. Red corresponds to mass excesses and blue corresponds to mass deficiencies (Image credit: NASA/JPL-Caltech/MIT/GSFC).*

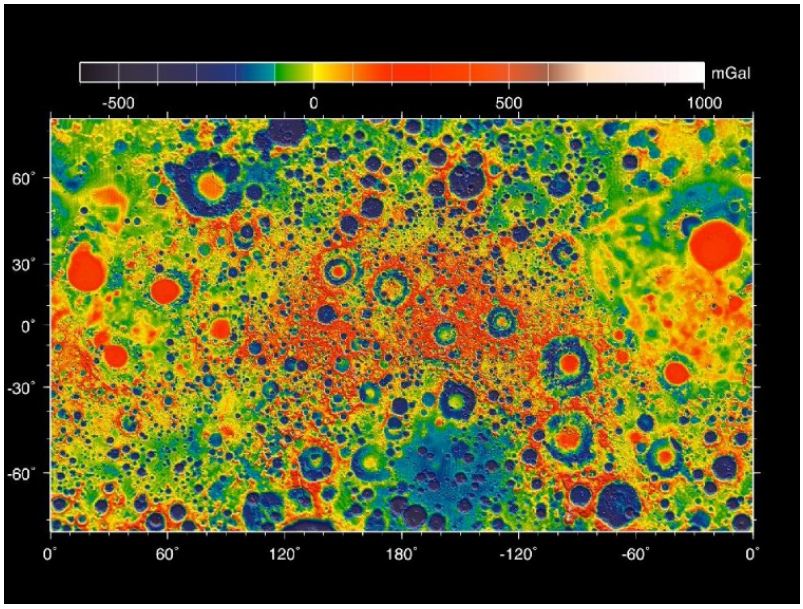


*Figure 4. Map of the gravity field of the moon as measured by NASA's GRAIL mission with the viewing perspective of Mercator projection. Reds correspond to mass excesses which create areas of higher local gravity, blues correspond to mass deficits which create areas of lower local gravity (Image credit: NASA/JPL-Caltech/GSFC/MIT).*

Investigations of worldwide gravity and topography information suggest that the thickness of the far side outside surpasses that of the close to side by around 15 km all things considered, however the gravity-based outcomes are model dependent, and it is conceivable to develop models with along the side changing crustal piece that don't uncover huge contrasts in crustal thickness between the close and farsides of the hemisphere (Wieczorek, (2006) as cited in Jaumann et al., 2012). Numerous inquiries stay open with respect to the current constitution, inception, and evolution of the Moon that would best be addressed in the frame of a network mission.

## 3.4. Lunar Magnetism

The Moon has a magnetic field that is quite different from that of the Earth, that it lacks a global magnetic field and instead has extensive crustal magnetism, that, the average strength of the Moon's magnetic field is about 8 nT while that of the Earth is ~ 25-65 μT. According to the Lin, (1988) as cited in (Tiedeken, 2017), the Moon's magnetic field is about 10000 times weaker, in addition, solar wind provides an ambient magnetic field strength ~ 5-10 nT, Samples returned from the Apollo missions have shown that the main ferromagnetic carriers on the Moon consist of microscopic metallic iron particles in the reducing lunar environment. Regions antipodal to four of the largest lunar impact basins – Imbrium, Orientale, Crisium, and Serenitatis – have some of the strongest magnetic field concentration on the Moon. The most prominent of these is the region corresponding to the antipodes of the Imbrium and Serenitatis impact basins, which have surface fields greater than 40 nT, additionally, the high concentration of strong anomalies on the south-central farside of the Moon coincides with the northern rim of the South Pole-Aitken basin, which is the oldest and largest distinguishable lunar basin. The Imbrium basin itself corresponds to the largest concentration of weak surface fields (<0.2 nT) (Hood, (2013), as cited in (Tiedeken, 2017).

## 3.5. Remote sensing of the Moon

### 3.5.1. Definition of Remote sensing of the Moon

Remote detecting is the most incredible asset in present day planetary science and over ongoing years, has given the absolute most significant information that we hold of the Moon. Remote sensing data from the Clementine, Lunar Prospector, Chandrayaan and SELENE missions have now given a worldwide perspective on the arrangement of the lunar surface, also, they have given us an increasingly complete perspective on the shape, mineral composition, gravity and magnetic

anomalies related with the Moon. According to (Wright et al., 2012), estimations of the electromagnetic spectrum are just viable inside certain wavelength regions, as they give explicit analytic data going from atomic/molecular connections to physical properties of surface materials. Some wavelength regions valuable for diagnostic compositional investigation of the surface utilizing distantly detected information might be obscured by assimilation or disperse in the atmosphere of the planetary body being watched. Remotely sensed satellite stereo data are useful for extracting elevation through stereo data processing, as well as from active techniques such as radar and laser altimetry. The latter can produce high resolution DTMs that provide 3-dimensional geospatial visualization and characterization of topographic features such as impact and volcanic related structures. Elevation information can likewise be joined with different datasets to make 3D representations that encourage connections with spectral units or potentially high-resolution morphologic units, and furthermore for understanding of structural/stratigraphic connections (Wright et al., 2012).

### 3.5.2. Remote sensing techniques

#### 3.5.2.1. Photogeology

Photogeology is the utilization of aerial or orbital information to interpret geological and geomorphologic highlights. Geologists have utilized aerial photos for a considerable length of time to decide rock presentations from surfaces with and without vegetation, study the declaration of landforms for understanding into their sources (geomorphology), determine the structural arrangements of disturbed bedrock, evaluate dynamic changes from natural events (for example floods; volcanic eruptions), and use as a visual base guide, normally related to topographic maps, on which a more detailed map can be derived (Wright et al., 2012).

#### 3.5.2.2.Reflectance Spectroscopy

The utilization of remotely acquired spectra of planetary surfaces for geologic investigations has expanded significantly in the most recent decade. Spectral data have been utilized to distinguish minerals on the earth and on all the solid surfaces in the nearby planetary group just as well as composition of atmospheres when present. The reflectance range of a particulate surface is eccentric, being affected by the number and kind of materials present, their weight divisions, the grain size of each material, and the survey geometry (Clark & Roush, 1984). According to (Dunkin & Heather, 2000), the high spectral resolution of the telescopic data enables accurate determination

of relative abundances of specific minerals (i.e. pyroxenes vs, olivines), however the poor spatial goals of a couple of kilometers on the ground, best case scenario restricts the utilization of the systems to bigger scale contemplates. Adjustable reflectance information has been utilized in this style to demonstrate compositional varieties crosswise over highlights, for example, the bigger new effect pits and the maria. These gave a portion of the primary signs with regards to the general piece of the lunar outside layer and maria away from the Apollo and Luna testing station.

#### 3.5.2.3.Gamma ray and X-ray spectroscopy

X-ray and gamma-ray remote sensing perceptions find significant applications in the investigation of the advancement of the planets out of the primitive solar nebula. Orbital estimations can be completed on nearby planetary group bodies whose atmospheres and caught radiation conditions do not interfere altogether with the emissions. Elemental compositions can be deduced from perceptions of these line emissions. Gamma-ray emissions can be ascribed primarily to natural radioactivity (Th, U and K) and to primary and secondary cosmic ray-induced activity producing identifiable emissions from, for instance, H, O, Si, Al, Mg, Fe, Ti and Ca. The significant radiation source for remote orbital X-ray spectroscopy is that delivered by characteristic X-rays following the interaction of solar based X-rays with the surface of the irradiated planetary system bodies (Trombka et al., 1999). X-ray fluorescence spectroscopy has for quite some time been utilized in researches to decide essential elemental abundances in rock and oil tests. In this method, an X-ray source is utilized to launch electrons from the atoms at the surface of the example, offering ascend to the discharge of monoenergetic X-rays with energies characteristic to the components present. The energies included range somewhere in the range of 0.1 and 100keV, testing just the upper ten of microns of the surface being referred to. This strategy was utilized for remote sensing for an enormous scale during the Apollo 15 and 16 missions (Dunkin & Heather, 2000).

## 3.6. An approach to terraforming the Moon

### 3.6.1. Terraforming

The word terraforming literally translates to the "Earth-shaping" of a planet, moon, or other celestial body, it is theoretical procedure of purposely adjusting its atmosphere, temperature, surface topography or ecology to be similar to the environment of Earth to make it tenable by Earth-like life. As cited in (Pazar, 2018) according to (Fogg & Hiscox (2001), Moores & Melo, (2003), terraforming is the international application of anthropogenic forcing to a planetary environment in order to effect a desired climactic change, and the term terraforming was begat by the science fiction writer Jack Williamson in a sci-fi short story. The long timescales and practically of terraforming are the subject of debate. Other unanswered inquiries identify with the morals, coordinations, financial aspects, legislative issues, and strategy of changing nature of an extraterrestrial world, and the ability of a spherical planetary body to be technologically transformed depends mostly on its initial conditions of astrophysical, atmospheric, and geologic parameters (Pazar, 2018).

### 3.6.2.Terraforming technologies and climate change

Theoretical technologies and modern technologies are the two distinct gatherings of terraforming or planetary designing related innovation. For our hypothetical showing of the progression and credibility of terraforming a planet or moon, (Pazar, 2018), expects that the vital innovation is both obtained and used, without confinement of recourses, and that it follows the money related improvement twist from before that relies in the long run upon population growth. According to (McKay, (2008) as cited in Pazar, 2018), terraforming will in the long run be encouraged through a blend of these sorts of super scale engineering and biological planetary building advancements and the ultimate objective is explicitly aimed at improving the limit of an extraterrestrial planetary condition to accomplish livability and making an open planetary biological system that is equipped for self-guideline.

### 3.6.3.Terraforming the Moon

The main problem facing the colonization and sustainability of the Moon is low gravity, which presents the challenge of the ability to retain an atmosphere. First approach to terraforming the Moon, would be dealing with the atmosphere which is so thin it is just about the layer of the earth's

atmosphere which is exosphere. According to (Beech, 2009), the Moon's exosphere contains, at any one instance, about 10,000 kg of gas. To make an expanded lunar atmosphere, accordingly, the current exosphere mass must be expanded by about 10000 times. Given that the solar wind mass-loss rate tops at around 100 kg/s, it maybe bodes well to develop the Moon's climatic mass at this equivalent rate. It has been evaluated that any gases that may be brought into the Moon's exosphere will be lost inside a matter of few weeks. This problem can be addressed by several ways, including the industrial heating of lunar regolith material, through subsurface nuclear bomb mining and one of the is iceteroid bombarding. In order to perform ice bombarding, comets made up of water ices must be captured, known as iceteroids and bombard our moon's surface with at least hundreds of those comets. On colliding with the moon's surface, they would amass on its surface to shape common assortments of ice. Plus, these comets would scatter carbon-di-oxide, water fume, and modest quantities of ammonia and methane. These gases would provide the required atmosphere to our satellite. The transfer of these comets would also cause the moon to gain momentum, and thus, the Moon would start rotating more rapidly due to the faster rotation, it would no longer be tidally locked to earth. It would gain earth-like rotation. A Moon with an artificial atmosphere will be another world for people to live upon and to investigate. It will likewise be another Moon, truly, for the individuals who stay on the Earth, since the artificial atmosphere, whenever built up, will bring about an a lot more splendid intelligent sparkle than it shows right now (Beech, 2009).

## 3.7. Methods used to determine the volume and density of the rocks

### 3.7.1. Photogrammetry

Photogrammetric systems, estimating objects from photos, have been used since the late 1800s. These strategies are most regularly utilized for mapping enormous zones from aeronautical photos. Computerized short proximity photogrammetry is a system for precisely estimating items legitimately from photos or advanced pictures caught with a camera at short proximity. According to (Tüdeş, (1996) as cited in (Yakar & Yilmaz, 2008), numerous, covering pictures taken from alternate points of view, produces estimations that can be utilized to make exact 3D models of objects, thus, knowing the position of camera is not necessary because the geometry of the object is built up legitimately from the pictures.

According to the (Yakar & Yilmaz, 2008), photogrammetric 3D arrange assurance depends on the co-linearity condition which just expresses that, camera projective focus and picture point lie on a straight line. The determination of the 3D coordinates from a positive point is accomplished through the crossing point of at least two straight lines. In this way, each focal point ought to show up in any event two photos. Afterward, coordinates are estimated from 3D model which is established by photogrammetric programming.

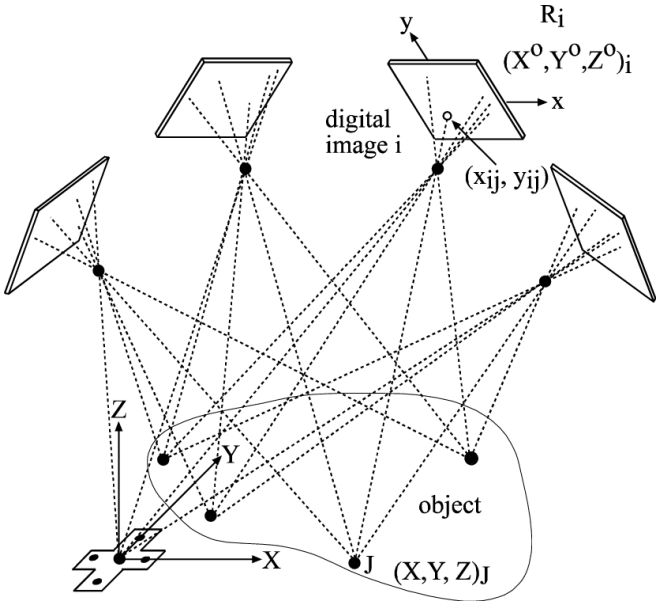


*Figure 5. Convergent close-range photogrammetric network comprising four camera stations (Ryall & Fraser, 2002).*

Close-range photogrammetry is productive and quick, essentially less time consuming to gather information in the field. Digital close-range photogrammetric methods have been successfully applied to projects in archaeology, architecture, automotive and aerospace engineering, accident reconstructions, that, according to (Yakar et al., 2010), similar procedure can be utilized to get dimensional estimations productively on inaccessible structures, for example, tunnels and dams, and enormous or complex buildings. Computerized photogrammetric estimations can be fused with 3D displaying and figuring out procedures. The obtained information is interminable and the cost savings substantial.

### 3.7.2.X-ray Fluorescence

XRF is analytical method to determine the chemical composition of all kinds of materials and the materials can be in solid, liquid, powder filtered or other form. XRF can also sometimes be used to determine the thickness and composition of layers and coatings. This strategy is quick, precise and non-destructive, and for the most part requires just at least example readiness. Applications are wide and incorporate the metal, bond, oil, polymer, plastic and nourishment enterprises, alongside mining, mineralogy and geology, and natural investigation of water and waste materials (Brouwer, 2010).

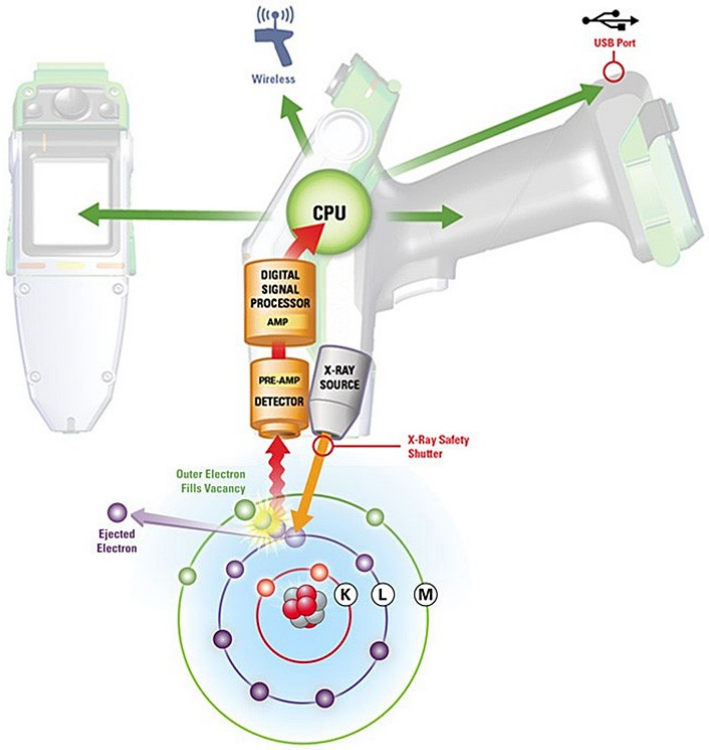


*Figure 6. Portable X-ray Fluorescence Instrument. https://www.thermofisher.com/cz/en/home/industrial/spectroscopy-elemental-isotope-analysis/spectroscopy-elemental-isotope-analysis-learning-center/elemental-analysis-information/xrf-technology.html).*

The chemical compositions of rocks are utilized to take care of various geological issues, including crystallization history of molten bodies, for example, stone or basalt, procedures of development of the ocean bottom, nature of compound enduring in different atmospheres, stratigraphic connection of sedimentary and volcanic rocks, procedures of metal age, and numerous others. Most

of the rocks are made essentially out of silicate minerals, and over 90% of the structure of most silicate rocks can be described by oxides of Si, Ti, Al, Fe, Mg, Ca, Na and K. Minor and these components present in rocks incorporate basically every other component, a significant number of which are particularly valuable for geochemical displaying of topographical procedures (Tour, 1989).

# 4. METHODOLOGY

## 4.1. Materials

In this study 5 rocks from Saratoga Springs in the United States were used. From the identification with naked eye, rocks are fine-grained marbles, or metamorphic limestones, and fine-grained quartzitic sandstone were used in this work.

## 4.2. List of techniques

In this part of the work, I demonstrated the usages of above-mentioned methods and imparted necessity software programs used for determining the data. Each rock was examined using two techniques and lastly the mass of the rocks computed by using the data's derived from those two techniques.

### 4.2.1. Volume computing photogrammetry

Volume computing photogrammetry technique was used to obtain the volume of the rocks. The calculation was completed with the help of the 3D generating digital close-range photogrammetry method. Program Agisoft Photoscan granted a clean, high-quality 3D models of the rock samples, thus, from the perfected 3D model by Agisoft, with the help of softwares Blender and 3DS MAX the volume of the rock samples was derived. The volumes supplied from 3D photomodels of samples would be compared with volumes calculated from classical technique. Further this computed volume will be used one of the components of the mass determination method.

### 4.2.2. Density determination by x-ray fluorescence

The chemical compositions of the rock pebbles were derived from the Vanta X-ray Fluorescence Analyzer. Further in the consequence of the obtained data, the density of the rock pebbles were determined by relation between specific gravity and the iron content of the rocks from the research paper of (Sheldon, 1964). The estimated density of the rock samples will be the second component of mass determination method.

#### 4.2.3.Used computer software programs and instruments

##### 4.2.3.1.Agisoft Photoscan

Agisoft PhotoScan version 1.3 was used for all image processing. “PhotoScan is an advanced image-based solution for creating three-dimensional content from still images”. PhotoScan is produced by the Russian company Agisoft and is built to operate on windows operating systems, but it also runs on Mac and Linux systems. There are some considerations when determining a system capable of running Photoscan. A 64-bit operating system with a multicore processor and a decent amount of RAM is strongly recommended. As soon as the computer runs out of main memory, it automatically switches to virtual memory slowing down processing time dramatically. The PhotoScan software takes a three-step processing approach according to (Agüera-Vega (2016) as cited in (Rhodes, 2017). The first step in this process is image alignment where photos are aligned resulting in a sparse point could, the camera locations, and calibration parameters. Next, the majority of scene details are built by applying Multiview stereo reconstruction on the previously aligned photos resulting in a dense point cloud. Finally, the mesh is generated and textured using the photographs.

##### 4.2.3.2.Blender

Blender is a 3D content creation program. It is open source software and free of charge, published under the GNU license by a non-profit organization: The Blender Foundation. That means, you do not need to purchase a license or ask for permission to use it for any kind of private or commercial projects. This software is used widely for creating animated films, visual effect, art, 3D printed models, interactive 3D applications and video games. Blender’s features include 3D modeling, UV unwrapping, texturing, raster graphics editing, rigging and skinning, fluid and smoke simulation, particle simulation, soft body simulation, sculping, animating, match moving, rendering, motion graphics, video editing and composing.

##### 4.2.3.3.X-ray Fluorescence Analyzer

For the field measurements X-Ray Fluorescence Analyzer from company Vanta Family have been used. The Vanta XRF analyzer is the most developed handheld X-ray fluorescence gadget and gives fast, exact component investigation and combination recognizable proof to clients who request research facility quality outcomes in the field.


*Figure 7. Vanta X-Ray Fluorescence Analyzer instrument (source: http://www.olympus-ims.com/en/vanta).*

## 4.3. Data processing

### 4.3.1. Volume data processing

The first mission has been to take a quality close-range of photos of the samples. Taking photographs has been done with Canon EOS 60-D in Canon EF 50mm f/1.8 STM lens (Fig. 7). Camera calibration procedures have been completed with mathematical calculations. Close ranged photographs were taken several times around, it was necessary to take the photos with no less than 70 percent overlap for each following photo. The methods for catching pictures should be adjusted relying upon the topic and circumstance. The photographs have been done in three type of circles (360°) and angles, from above, the other circle is where the photos had been taken perpendicular and the third circle is from below. Approximately, 60-70 photos had been taken per one sample rock.


*Figure 8. Camera and Lens which were used to take close range photographs, further taken photos were used in photogrammetry the Canon EOS 60-D and lens Canon EF 50mm f/1.8 STM.*

The taken photos has been left in RAW format, to adjust and edit the photos in photoshop in order to remove glares and shadows. Edited photographs were converted to .JPG format and imported to Agisoft PhotoScan software, that, the software will start making 3D model by matching points and doing sparse point cloud based on photo alignment.

*Figure 9. Photo of sample SS007D taken with Canon EOS 60-D 50mm f/1.8 STM lens.*

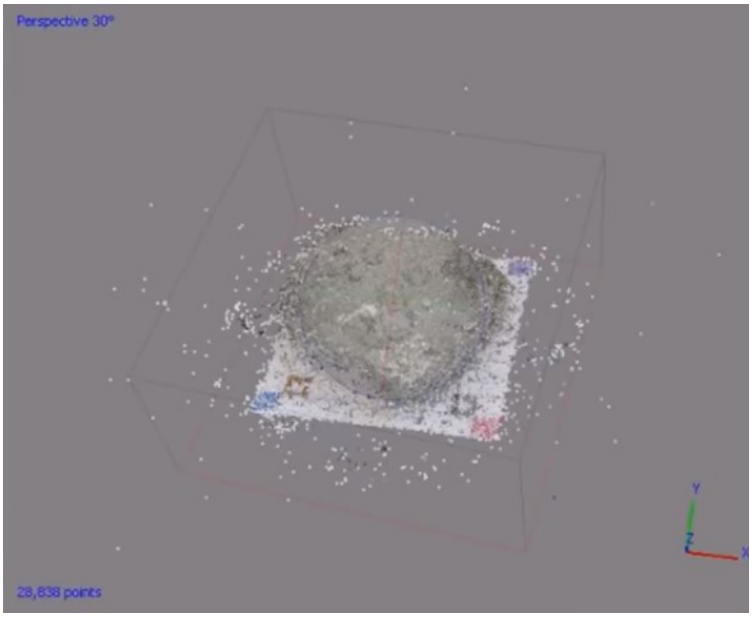


*Figure 10. Spare point cloud based on photo alignment by Agisoft PhotoScan software.*

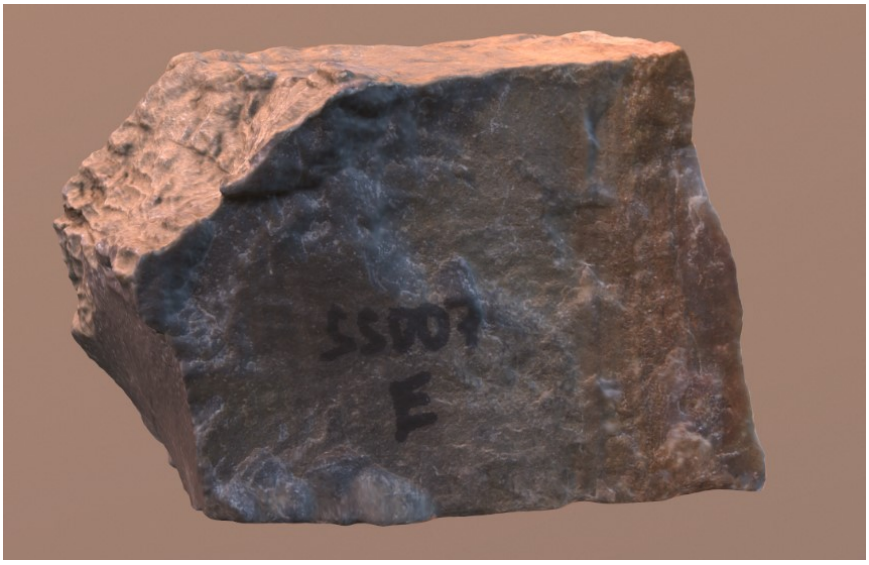


*Figure 11. 3D model of sample "SS007E" done by Author of the thesis using Agisoft Photoscan software.*

Volume was derived from the model which was made from software Agisoft Photoscan. The volume calculation has been done with the help of Blender software, by importing the perfect 3D model of the rock sample.

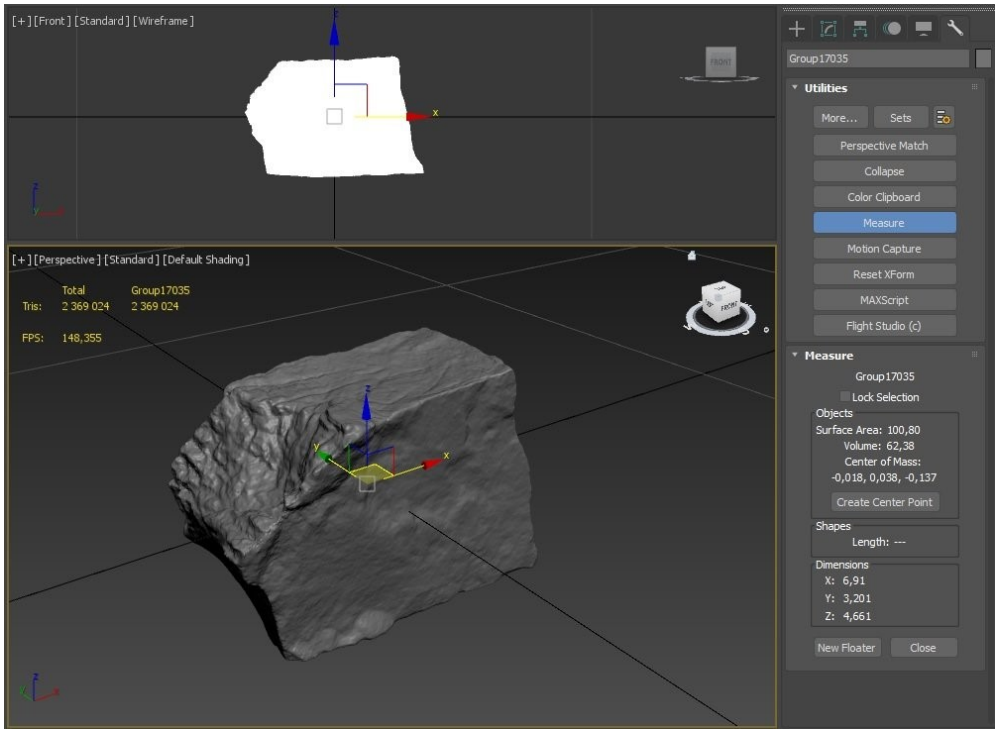


*Figure 12. Measured Volume of sample SS007E by Blender software.*

### 4.3.2.Density data processing

Density data, as earlier mentioned, was derived from chemical compositions (from Vanta X-ray fluorescence) by using relation between specific gravity and the iron content of the rocks. From measured chemical compositions of the rock samples, iron content (see Table 2) was used in order to compute the bulk specific gravity ($SG_b$), in other hand specific gravity is pore-less density and that is 1/pore-less density, according to the research work of (Sheldon, 1964).

*Table 2. Chemical compositions of rock samples from XRF.*

| | SS007A | SS007D | SS007E | SS007G | SS007H |
|---|---|---|---|---|---|
| Mg (%) | 4.829 | 1.076 | 1.744 | 1.828 | 3.474 |
| Al (%) | 4.304 | 4.064 | 0.536 | 3.816 | 2.491 |
| Si (%) | 24.06 | 25.94 | 2.2182 | 10.68 | 7.829 |
| K (%) | 5.807 | 4.034 | 0.1129 | 1.373 | 0.611 |
| Ca (%) | 5.530 | 0.532 | 27.7784 | 20.01 | 14.92 |
| Ti (%) | 0.197 | 0.302 | 0.023 | 0.044 | 0.148 |
| Mn (%) | 0.032 | 0.108 | 0.0346 | 0.082 | 0.167 |
| Fe (%) | 1.305 | 2.313 | 0.4427 | 1.638 | 1.058 |
| Sr (%) | 0.032 | 0.016 | 0.1389 | 0.018 | 0.0065 |

Iron content as highlighted in the Table 2 was then further used to determine the specific gravity (pore-less density) based on correlation chart (Figure 10) between iron content in percentage and reciprocal of bulk specific gravity.

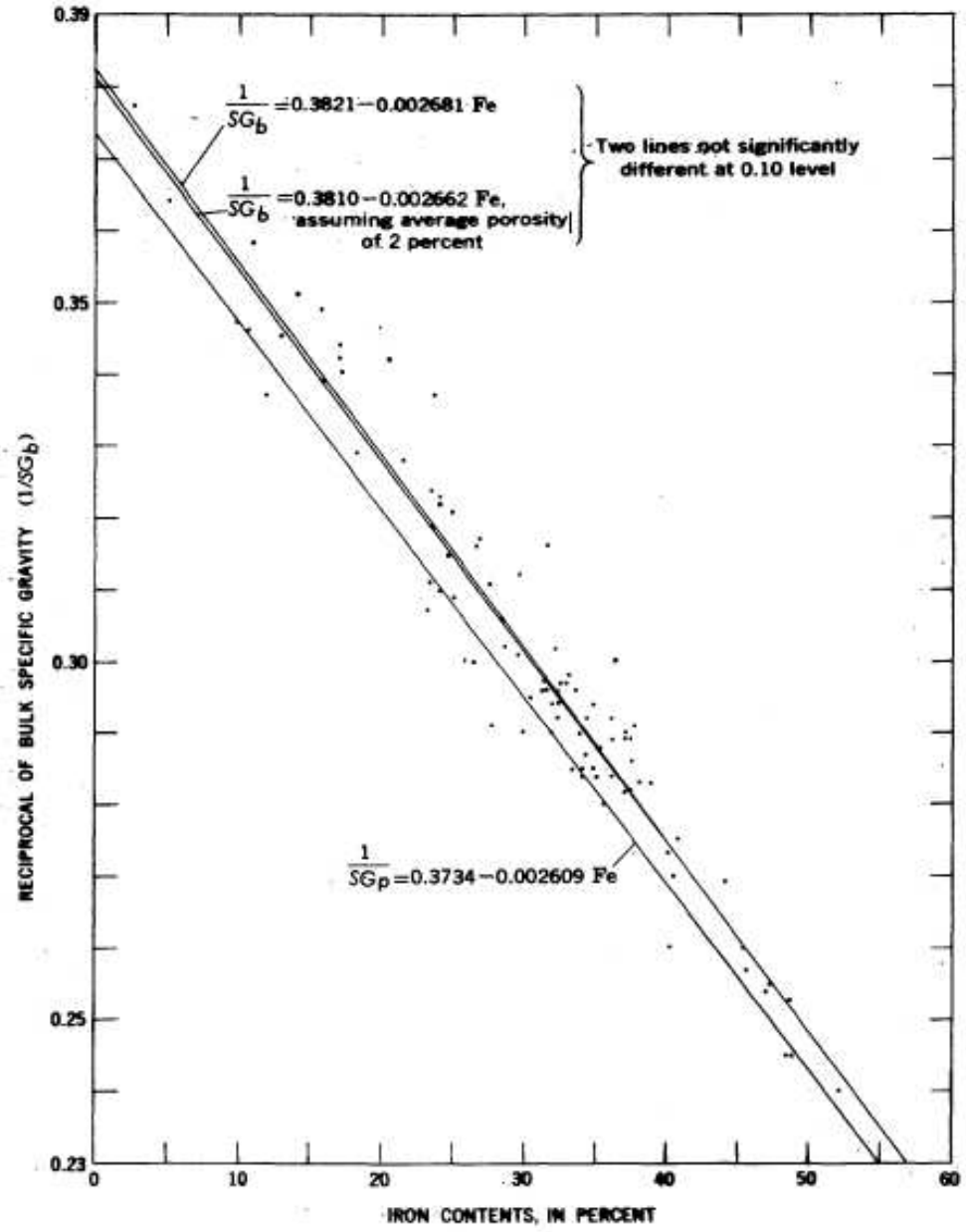


*Figure 13. Correlation between the reciprocal of the bulk specific gravity and the iron content (Sheldon, 1964).*

# 5. RESULTS AND DISCUSSION

This section focuses on the results and discusses these findings. The first part looks at the finding used in calculating volume using the 3D model in comparison to the classic method. The second part looks at results from analyzing data density of the rocks and lastly this work shows result from mass determination.

## 5.1. Volume data

With the advancement in innovation, computerized techniques such as close-range photogrammetry and with the improvement of equipment and programming software like Blender, results from volume estimation provided various level of success. Table 3 shows the results from the volume 3D model and volume calculated with the classic method Archimedes principle. As can be seen in the table below, the were minimum differences between the classic methods and the 3D model.

*Table 3. Results from volume calculations.*

| Object | Volume 3D model | Volume Classic Method |
|---|---|---|
| SS007A | 6.61 $cm^3$ | 6.5 $cm^3$ |
| SS007D | 25.16 $cm^3$ | 25.09 $cm^3$ |
| SS007E | 62.45 $cm^3$ | 62.51 $cm^3$ |
| SS007G | 11.27 $cm^3$ | 11.24 $cm^3$ |
| SS007H | 16.37 $cm^3$ | 16.46 $cm^3$ |

The Table 3 shows that the results from 2 different aspect of finding volume of an object, in this case, rock pebble samples from Saratoga Spring is not differing that much. It indicates, that the progression in computerized techniques can be as accurate as classic volume determinations, and are as efficient.

## 5.2. Density data

Density results that was derived from the chart of relation between iron content and specific gravity by using the chemical composition from X-ray fluorescence instrument gave different degree of accomplishment. The difference between the density results did not surpass 0.5 g/cm$^3$ which is 5% of iron content, however, when the iron content in the rock detected by X-ray fluorescence is low (e.g. <1%) the error in establishing the density is large. Table 4 demonstrates the consequences of the determined density. Despite absolute density is more accurate than the density derived from X-ray fluorescence, the differences in this study between the two techniques are minimum as shown in Table 4. As (Johnson et al., 1999), suggested that one of the many advantages in applying X-ray fluorescence (XRF) to the analysis of rocks and minerals, one of the most obvious is the versatility of the instrumentation.

*Table 4. Results of density from XRF, absolute density and error calculations.*

| Sample | Absolute density | Density from XRF |
|---|---|---|
| SS007A | 2.810 | 2.70 |
| SS007D | 2.407 | 2.73 |
| SS007E | 2.889 | 2.75 |
| SS007G | 2.325 | 2.71 |
| SS007H | 2.412 | 2.66 |

## 5.3. Mass determination

By using the two aforementioned techniques, we can go further to determine rock mass by using the formula:

$$M = V * \rho$$

Where:

V – Volume [$m^3$]

ρ – Density [$g/cm^3$]

Mass of the rock samples can be found in the Table 5. Hence, the weight of the studied samples can be determined from the multiplication of studied mass and gravitational acceleration of the planets which can be seen in the Table 6.

*Table 5. Computed mass of the samples.*

| Samples | Volume from 3D model ($m^3$) | Density from XRF ($g/cm^3$) | Computed Mass (g) |
|---|---|---|---|
| SS007A | 6.61 | 2.70 | 17.86 |
| SS007D | 25.16 | 2.73 | 68.93 |
| SS007E | 62.45 | 2.75 | 171.8 |
| SS007G | 11.27 | 2.71 | 30.62 |
| SS007H | 16.37 | 2.66 | 43.65 |

*Table 6. Weight distinctions of the samples on the different planetary surfaces in Newtons [N].*

| | Earth | Moon | Mars | Venus | Mercury | Jupiter | Saturn |
|---|---|---|---|---|---|---|---|
| SS007A | 0.175 | 0.028 | 0.067 | 0.158 | 0.064 | 0.463 | 0.197 |
| SS007D | 0.675 | 0.111 | 0.259 | 0.611 | 0.247 | 1.788 | 0.763 |
| SS007E | 1.684 | 0.278 | 0.648 | 1.524 | 0.617 | 4.460 | 1.904 |
| SS007G | 0.300 | 0.049 | 0.115 | 0.271 | 0.109 | 0.794 | 0.339 |
| SS007H | 0.427 | 0.070 | 0.164 | 0.387 | 0.156 | 1.132 | 0.483 |
| acceleration due to gravity (N/kg) | 9.8 | 1.62 | 3.77 | 8.87 | 3.59 | 25.95 | 11.08 |

From the foregoing, the results have shown that the use of the two techniques can help in determining rock mass. The efficiency and accuracy of these techniques can be used to evaluate and determine rock mass from other planetary bodies apart from earth.

# 6. CONCLUSION

This work set out to evaluate the rock mass on planetary bodies. Using 5 sample rocks, this work utilized two main techniques to evaluate rock mass and infer this on other planetary bodies.

The results in this bachelor's thesis showed that while using of these techniques to determine rock mass are not as accurate and they can be used to make approximate inferences of rock mass on other planetary bodies. The implication of these findings are for ways to colonise and terraform other planetary bodies: using of techniques such as photogrammetry and x-ray fluorescence can help us in gaining more understand of other planetary bodies. This understanding will help us accelerate in the process of colonising such bodies.

# 7. REFERENCES


Beech, M. (2009). Terraforming: the creating of habitable worlds. *Choice Reviews Online*. https://doi.org/10.5860/choice.47-0242

Bieniawski, Z. T. (1993). Classification of rock masses for engineering: the RMR system and future trends. *Comprehensive Rock Engineering. Vol. 3*. https://doi.org/10.1016/b978-0-08-042066-0.50028-8

Brouwer, P. (2010). Theory of XRF : getting acquainted with the principles. In *Almelo: PANalytical B.V.*

Burke, J. D. (1986). Lunar Materials and Processes. *National SAMPE Symposium and Exhibition (Proceedings)*.

Carmichael, R. S. (2017). Practical Handbook of Physical Properties of Rocks and Minerals (1988). In *Practical Handbook of Physical Properties of Rocks and Minerals (1988)*. https://doi.org/10.1201/9780203710968

Clark, R. N., & Roush, T. L. (1984). Reflectance spectroscopy: quantitative analysis techniques for remote sensing applications. *Journal of Geophysical Research*, *89*(B7), 6329–6340. https://doi.org/10.1029/JB089iB07p06329

Dunkin, S. K., & Heather, D. J. (2000). Remote Sensing of the Moon: The Past, Present and Future. *Estec*, *4*(January), 10–15. http://conferences.esa.int/Moon2000/index.html

Jaumann, R., Hiesinger, H., Anand, M., Crawford, I. A., Wagner, R., Sohl, F., Jolliff, B. L., Scholten, F., Knapmeyer, M., Hoffmann, H., Hussmann, H., Grott, M., Hempel, S., Köhler, U., Krohn, K., Schmitz, N., Carpenter, J., Wieczorek, M., Spohn, T., … Oberst, J. (2012). Geology, geochemistry, and geophysics of the Moon: Status of current understanding. *Planetary and Space Science*, *74*(1), 15–41. https://doi.org/10.1016/j.pss.2012.08.019

Johnson, D. M., Hooper, P. R., & Conrey, R. M. (1999). XRF analysis of rocks and minerals for major and trace elements on a single low dilution Li-tetraborate fused bead. *Advances in X-Ray Analysis*, *41*(C), 843–867.

Konopliv, A. S., Binder, A. B., Hood, L. L., Kucinskas, A. B., Sjogren, W. L., & Williams, J. G. (1998). Improved gravity field of the moon from lunar prospector. *Science*, *281*(5382), 1476–1480. https://doi.org/10.1126/science.281.5382.1476

McFadden, L. A., Weissman, P. R., & Johnson, T. V. (2007). Encyclopedia of the Solar System. In *Encyclopedia of the Solar System*. https://doi.org/10.5860/choice.44-5979

Pazar, C. C. (2018). *Terraforming of Terrestrial Earth-sized Planetary Bodies*. *February*, 1–62.

Rhodes, R. K. (2017). *UAS as an Inventory Tool: A Photogrammetric Approach to Volume Estimation*. http://scholarworks.uark.edu/etd/2424/

Sheldon, R. P. (1964). *lelation Between Specific ; ravity and Iron Content • f · Roc : ks . From the · Red r ' lountain Fo . rmation , Alabama*.

Singh, B., & Goel, R. K. (1999). Rock Mass Classification. A Practical Approach in Civil Engineering. In *Rock mass classification. A practical approach in civil engineering.*

Steinberger, B., Zhao, D., & Werner, S. C. (2015). Interior structure of the Moon: Constraints from seismic tomography, gravity and topography. *Physics of the Earth and Planetary Interiors*, *245*, 26–39. https://doi.org/10.1016/j.pepi.2015.05.005

Tiedeken, S. L. (2017). *Magnetism and geology of the moon*.

Tour, T. E. L. A. (1989). *Contributed Papers Analysis of Rocks Using X-Ray Fluorescence Spectrometry*. *6*(1), 3–9.

Trombka, J. I., Evans, L. G., Starr, R., Clark, P. E., & Floyd, S. R. (1999). Future planetary X-ray and gamma-ray remote sensing system and in situ requirements for room temperature solid state detectors. *Nuclear Instruments and Methods in Physics Research, Section A: Accelerators, Spectrometers, Detectors and Associated Equipment*. https://doi.org/10.1016/S0168-9002(99)00007-8

Wirnsberger, H., Krauss, S., & Mayer-Gürr, T. (2019). First independent Graz Lunar Gravity Model derived from GRAIL. *Icarus*, *317*(May 2018), 324–336. https://doi.org/10.1016/j.icarus.2018.08.011

Wright, S. P., Tornabene, L. L., & Ramsey, M. S. (2012). Remote Sensing of Impact Craters.

*Impact Cratering: Processes and Products*, 194–210. https://doi.org/10.1002/9781118447307.ch13

Yakar, M., & Yilmaz, H. M. (2008). Using in Volume Computing of Digital Close Range. *The International Archives of the Photogrammetry, Remote Sensing and Spatial Information Sciences. Vol. XXXVII*, *C*(Patikova), 119–124.

Yakar, M., Yilmaz, H. M., & Mutluoglu, O. (2010). Close range photogrammetry and robotic total station in volume calculation. *International Journal of Physical Sciences*, *5*(2), 086–096.